NJC

Accepted Manuscript

This is an *Accepted Manuscript*, which has been through the Royal Society of Chemistry peer review process and has been accepted for publication.

Accepted Manuscripts are published online shortly after acceptance, before technical editing, formatting and proof reading. Using this free service, authors can make their results available to the community, in citable form, before we publish the edited article. We will replace this *Accepted Manuscript* with the edited and formatted *Advance Article* as soon as it is available.

You can find more information about *Accepted Manuscripts* in the Information for Authors.

Please note that technical editing may introduce minor changes to the text and/or graphics, which may alter content. The journal's standard Terms & Conditions and the Ethical guidelines still apply. In no event shall the Royal Society of Chemistry be held responsible for any errors or omissions in this *Accepted Manuscript* or any consequences arising from the use of any information it contains.

ROYAL SOCIETY OF CHEMISTRY

www.rsc.org/njc

New Journal of Chemistry

ARTICLE

Influence of Main-chain and Molecular Weight on the Phase Behaviors of Side-Chain Liquid Crystalline Polymers without the Spacer

Received 00th January 20xx,
Accepted 00th January 20xx

DOI: 10.1039/x0xx00000x

www.rsc.org/

Ni Bin, Luo Yongbin, Liu Yujie, Chen Sheng*, Zhang Hailiang*

A series of end-on side-chain liquid crystalline polymers (SCLCPs) based on biphenyl mesogen, poly(4, 4'-alkoxybiphenyl acrylate) (PBiA-m, m = 1, 4, 6, 10, 18) were successfully synthesized by free radical polymerization or reversible addition fragmentation chain transfer (RAFT) polymerization. The chemical structures of the monomers were confirmed by ^{1}H NMR and Mass Spectrometry. The phase structures and transition behaviors were studied using DSC, POM and 1D WAXD. The experimental results found that PBiA-m showed the bilayer smectic phase and the higher clearing point (T_i), compared with the poly(4, 4'-alkoxybiphenyl methacrylate) (PBiMA-m). In addition, poly(4, 4'-hexyloxybiphenyl methacrylate) (PBiMA-6) and poly(4, 4'-hexyloxybiphenyl acrylate) (PBiA-6) with different molecular weights (M_n) and low molecular weight distributions have been successfully synthesized via RAFT polymerization. The results indicated that all polymers exhibited the bilayer smectic phase and the T_i increased as the M_n of PBiMA-6 and PBiA-6 increased. Moreover, the PBiA-6 had a higher T_i, compared with the PBiMA-6 with the similar M_n. All of those results suggested that the main-chain (acrylate and methacrylate) and M_n had a great influence on the properties of SCLCPs without the spacer.

1. Introduction

Side-chain liquid crystalline polymers (SCLCPs) have attracted considerable attention not only because they showed the wide-range of potential application but also they provided a demanding challenge to our understanding of the molecular factors that promote self-organization in condensed phases.[1-6]

It is well-known that the first attempt to synthesize thermotropic LCPs date only to the beginning of the 1970s.[7] It is in this period, that on the background of vital interest and extensive practical utilization of low-molecular liquid crystals, publications revealing various approaches towards synthesis of thermotropic polymers LC systems begin to appear and mesomorphic polymers become the object of intensive attention of scientists, working in the field of polymer science.[8] Primitively, the people tied to directly link the mesgoen to the main-chain.[9,10] However, some end-on SCLCPs couldn't form the LC phase structure, for example, the poly(p-biphenyl methacrylate) and poly(cholesteryl acrylate) were amorphous.[10,11] Later, in order to resolve this problem, "decoupling concept" was proposed by Ringsdorf and Finkelmann, in which the flexible spacers were purposefully introduced to decouple the dynamics of the polymeric backbone and the mesogenic side-chain to maintain the liquid crystallinity of side-chains.[12,13] Since then, the "decoupling concept" has become a useful guideline for the molecular design of SCLCPs.[14-20] Therefore, a SCLCP comprises four distinct structural units: the main-chain, the spacer, the mesogenic group and the tail.[21, 22] For the main-chain, many scientific researchers pay attention to the effect of backbone flexibility on the transitional behavior of SCLCP, such as the polystyrene, polyacrylate, polymethacrylate, polynorbornene, poly(vinyl ether), polysiloxane, polyacetylene, polythiophene. Among these polymers, extensive research has been focused on acrylate or methacrylate based polymers for the ease of monomer synthesis and polymerization. On the other hand, they can be polymerized by living polymerization techniques, such as atom transfer radical polymerization (ATRP), reversible addition-fragmentation chain transfer (RAFT), nitroxide-mediated radical polymerization, which allow more precise studies to be undertaken to establish the role of the molecular structure with respect to the thermal and physical properties of SCLCP polymers.[23] For the spacer, highly or even completely decoupled end-on SCLCP can be realized when the length of the spacer was long, resulting in that the main-chain has little influence on the phase structure of the polymers because of the microphase separation.[24-25]

When the mesogenic side-chain attached to the main-chain without the flexible spacer, a strong "coupling effect" occurs in the main-chain and the mesogen. This "coupling effect" resulted in that the nature of the main-chain was very important in determining whether or not a polymer could display thermotropic mesophases.

Key Laboratory of Polymeric Materials and Application Technology of Hunan Province, Key Laboratory of Advanced Functional Polymer Materials of Colleges, Universities of Hunan Province, College of Chemistry, Xiangtan University, Xiangtan 411105, Hunan Province, China. Email: huaxuechensheng@163.com, zhl1965@xtu.edu.cn

For example, the poly(p-biphenyl acrylate) could form the LC phase, while the poly(p-biphenyl methacrylate) couldn't exhibit the LC phase.[10] Although the polymers contained the same mesogen, the phase structure of them was absolutely different. The people were aware of the influence of the main-chain on the phase behavior and structure of end-on SCLCPs without spacer, however, there has been few systematically studied on the properties of them. In addition, we considered that, comparison with the synthesis of SCLCPs with the spacer, it was easier to synthesize the SCLCPs when the mesgoens were introduced into the polymer backbone, meanwhile the polymers exhibited the stable phase structure because of the "coupling effect", which was of great importance for real applications. At present, our group is having exploited its real applications, such as solid-solid phase transition polymer materials.[26]

Except the chemical structure, the phase behavior of a SCLCP was also influenced by the degree of polymerization. There are numerous studies to focus on the relationship between M_n and phase behavior of SCLCPs with the flexible spacer in order to prepare polymers with predictable molecular weight and low non-uniformities by a well-defined synthetic approach.[27-29] The results showed that, one hand, the temperature range of the mesophase was enlarged with the increase of the M_n. The other hand, the number of mesophases and the nature of the mesophase both changed by increasing M_n. For example, Tomikawa et al. have reported that poly(6-[4-(4'-cyanophenyl)phenoxy]hexyl acrylate)s (PA6CB) with M_n lower than 2×10^4 g mol^{-1} exhibited the re-entrant nematic, smectic A and the nematic phase as temperature increased, while ones with M_n higher than 2×10^4 g mol^{-1} formed only nematic phase.[28] Percec et al have found out that 8-[(4-cyano-4'-biphenyl)oxy]octyl vinyl ether (6-8) with a degree of polymerization of 2.1 displayed an enantiotropic S_A and an enantiotropic nematic mesophase. Poly(6-8)s with degrees of polymerization from 4.2 to 10.2 displayed an enantiotropic S_A mesophase. Poly(6-8)s with degrees of polymerization larger than 12.4 displayed an enantiotropic S_x and an enantiotropic S_A mesophase.[30] Therefore, the polymer length is one of the significant factors affecting phase behavior in LC polymers. However, to the best of our knowledge, SCLCPs without spacer with different molecular weights has been no reported so far.

In this paper, we have described a detail study of the LC behavior of a series of end-on SCLCPs based on acrylate main-chain, poly(4, 4'-alkoxybiphenyl acrylate) (PBiA-m, m = 1, 4, 6, 10, 18, m is the length of alkyl tails). The other hand, we have systematically researched the relationship between phase behavior and M_n of poly(4, 4'-hexyloxybiphenyl methacrylate) (PBiMA-6) and poly(4, 4'-hexyloxybiphenyl acrylate) (PBiA-6) based on RFAT. Through studying, we can obtain some knowledge about the thermal behavior and the arrangement mode of molecular chain of PBiA-m, and can get the information of the SCLCPs without spacer and pocking mode molecular chain, can understand the influence of M_n on the properties of end-on SCLCPs without the spacer.

2. Experimental

2.1 Materials

Anhydrous tetrahydrofuran (THF) was distilled from sodium benzophenone ketyl under argon and used immediately. 2, 2 azobisisobutyronitrile (AIBN) was freshly recrystallised from methanol. 4, 4'-diphenol (98%, Alfa Aesar), acryloyl chloride, bromoalkanes together with other reagents and solvents were used as received without further purification.

2.2 Synthesis of monomers

For convenience, the 4, 4'-alkoxybiphenylyl acrylate monomers were named MBiA-m (m = 1, 4, 6, 10, 18), and the corresponding polymers were named PBiA-m. The synthetic route of monomers MBiA-m was shown in **Scheme 1**. The detailed synthetic procedures are described in supporting information.[31]

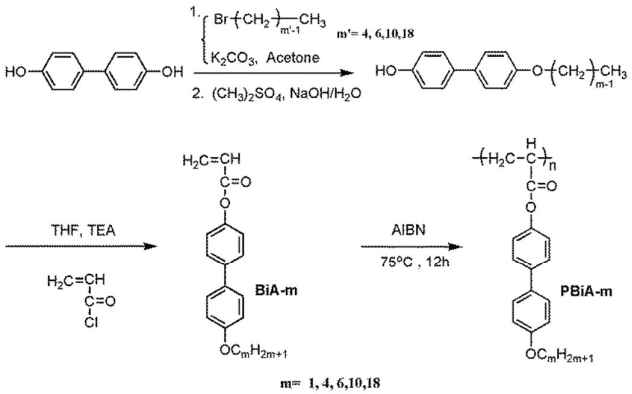

Scheme 1 Synthetic route of monomers (MBiA-m) and corresponding polymers (PBiA-m).

2.3 Synthesis of polymers

All polymers (PBiA-m) were obtained by conventional solution radical polymerization (see **Scheme 1)**, typically carried out as described in the following example.

The monomer, AIBN and THF were added into a dried reaction tube containing a magnetic stirrer bar. The molar ratio was set with $N_{monomer} : N_{AIBN} = 100 : 1$, and the monomer mass concentration was 25%. After three freeze-pump-thaw cycles, the tube was sealed under vacuum. Polymerization was carried out at 70 °C over 5 h. Then the white precipitate occurred in the tube. This kind of white solid couldn't be dissolved in the common solvent, such as $CHCl_3$, acetone, THF, petroleum ether and so on. In order to remove the residual monomers, the samples were purified by re-washing three times from the hot acetone.

The polymers, poly(4, 4'-hexyloxybiphenyl methacrylate) (PBiMA-6) and poly(4, 4'-hexyloxybiphenyl acrylate) (PBiA-6) were synthesized by RAFT polymerization (see **Scheme 2**). Polymerizations were conducted at 70 °C, using AIBN as the primary radical source and 1-cyano-1-methylethyl dithiobenzoate (CPDB) which was prepared according to the literature procedure as the RAFT chain transfer agent (CTA).[32] The molar ratio was set with $N_{AIBN} : N_{CPDB} : N_{monomer} = 1: 5: n$, n is the designed degree of polymerization and all the reaction time was 4 h. A typical polymerization procedure was as follows: MBiMA-6 (0.4 g, 1.1×10^{-3} mol), AIBN (0.0039 g, 2.4×10^{-5} mol), CPDB (0.0211 g, $1.2 \times$

10^{-4} mol) and chlorobenzene were added to a reaction tube. The mixture was degassed by four freeze-pump-thaw cycles and sealed under vacuum. The polymerization was carried out at 70 °C for 4 h and stopped by exposing to air. The polymerization solution was diluted with THF, followed by slowly precipitating from large amount of methanol. A red solid product was obtained after drying under vacuum at 50 °C. These polymers were named as PBiMA-6(1) ~ PBiMA-6(7) for PBiMA-6 and PBiA-6(1) ~ PBiA-6(6) for PBiA-6 (**Table 1**).

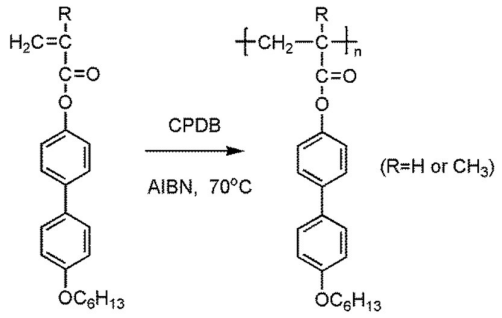

Scheme 2 Synthetic route of PBiMA-6 and PBiA-6.

2.4 Instruments and measurements

Nuclear magnetic resonance (NMR). ^{1}H NMR measurements were performed on a Bruker ARX400 MHz spectrometer using with $CDCl_3$ as solvent, tetramethylsilane (TMS) as the internal standard at room temperature.

Gel permeation chromatography (GPC). The apparent number average molecular weight (M_n) and polydispersity index (PDI = M_w/M_n) were measured on a GPC (WATERS 1515) instrument with a set of HT3, HT4 and HT5. The μ-styragel columns used THF as an eluent and the flow rate was 1.0 mL min^{-1} at 38 °C. The GPC data were calibrated with polystyrene standards.

Thermogravimetric analysis (TGA). TGA was performed on a TA SDT 2960 instrument at a heating rate of 20 °C min^{-1} in nitrogen atmosphere.

Differential scanning calorimetry (DSC). DSC traces of the polymer were obtained using a TA Q10 DSC instrument. The temperature and heat flow were calibrated using standard materials (indium and zinc) at a cooling and heating rates of 10 °C min^{-1}. The sample with a typical mass of about 5 mg was encapsulated in sealed aluminum pans.

Polarizing optical microscope (POM). LC texture of the polymer was examined under POM (Leica DM-LM-P) equipped with a Mettler Toledo hot stage (FP82HT).

One-dimensional wide-angle X-ray diffraction (1D WAXD). 1D WAXD experiments were performed on a BRUKER AXS D8 Advance diffractometer with a 40 kV FL tubes as the X-ray source (Cu Kα) and the LYNXEYE_XE detector. Background scattering was recorded and subtracted from the sample patterns. The heating and cooling rates in the 1D WAXD experiments were 10 °C min^{-1}.

A Rheometrics ARES rheometer (TA ARES rheometer). TA ARES rheometer was applied to measure the viscoelastic properties of the samples based on oscillatory shear. The experimental temperature was controlled using forced N_2 gas convection. Isochronal temperature scans were performed using a 20 mm diameter parallel-plate geometry with a frequency of 10 rad s^{-1} and a small strain amplitude. Isothermal frequency sweeps were made using the same setup at frequencies from 0.1 to 100 rad s^{-1}.

3. Results and discussion

3.1 Synthesis and characterization of monomers and polymers

A series of acrylate biphenyl monomers with the different lengths of alkyl tail (m = 1, 4, 6, 10, 18) were synthesized according to the synthetic route illustrated in Scheme 1. **Fig.1** (a) gives the ^{1}H NMR spectra ($CDCl_3$) of the monomer MBiA-10. The MBiA-10 showed the characteristic resonances of the vinyl group at 6.02, 6.30 and 6.63 ppm. In addition, the chemical shifts and peak integrations of all the protons in the monomers were in excellent agreement with its expected structure. Mass Spectrometry spectrums further confirmed the molecular structure (see **Fig.1** (b)). For the polymers PBiA-m (m = 1, 4, 6, 10, 18), the molecular characteristics were difficultly detected via ^{1}H NMR and GPC due to the insolubility. However, the polymers could dissolve in the common solvent when they were synthesized by RAFT via controlling the low degree of polymers. The GPC curves of PBiA-m were shown in **Figure S1** and the results were listed in **Table S1.** When the designed degree of polymer was 100, the polymers would separate out from the reaction solution after two hours. These indicated that the chain length has greatly effect on the solubility of PBiA-m. This phenomenon has never appeared in the SCLCPs with the spacer. Figure 1 (c) presented the ^{1}H NMR spectra ($CDCl_3$) of the polymer PBiA-10. After polymerization, vinyl group signals disappeared completely and the chemical shifts were quite broad and consistent with the expected polymer structure.

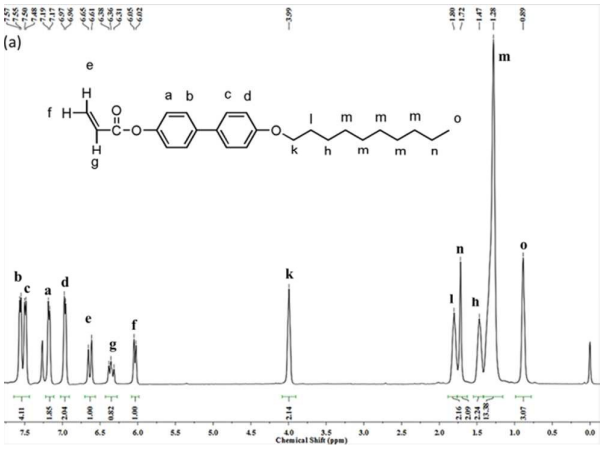

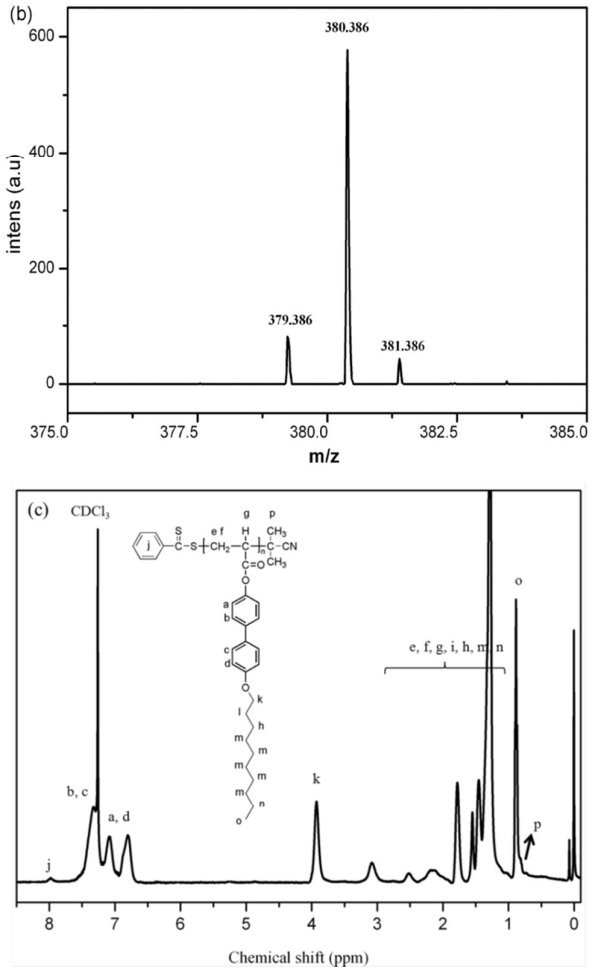

Fig.1 ^{1}H NMR spectrums (a) and MS spectrums (b) of the monomer MBiA-10 in $CDCl_3$. ^{1}H NMR spectrums of the polymer PBiA-10 in $CDCl_3$ (c).

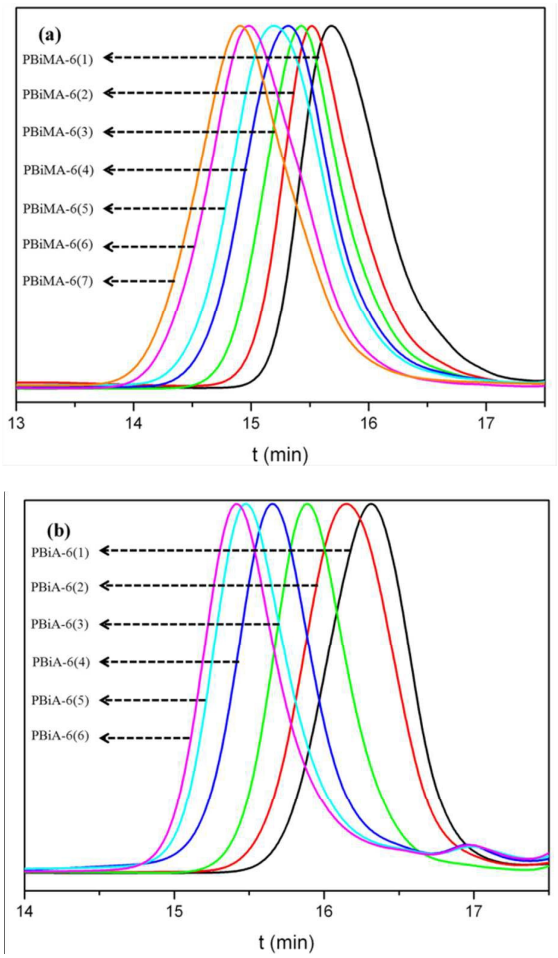

Fig.2 GPC trace of PBiMA-6(1)~PBiMA-6(7) (a) and PBiA-6(1)~PBiA-6(6) (b).

The polymers (PBiMA-6 and PBiA-6) with different M_ns were successfully synthesized by RAFT and GPC curves of PBiMA-6 and PBiA-6 were shown in **Fig.2** (a) and (b), respectively. As observed, the elution time shifted toward higher M_ns, the GPC traces remained monomodal and no shoulders existed after polymerization, showing the controlled "living" free radical polymerization. The GPC results were summarized in Table 1 and the M_n of polymers increased from 3.08×10^3 to 9.73×10^3 g mol^{-1} for PBiMA-6 and from 1.73×10^3 to 5.47×10^3 g mol^{-1} for PBiA-6.

Table 1 Molecular Characteristics of PBiMA-6(1) ~ PBiMA-6(7) and PBiA-6(1) ~ PBiA-6(6).

Sample(1)	$M_n(\times 10^3)^a$	PDI[a]	Sample(2)	$M_n(\times 10^3)^a$	PDI[a]
PBiMA-6(1)	3.08	1.29	PBiA-6(1)	1.73	1.16
PBiMA-6(2)	4.16	1.24	PBiA-6(2)	2.01	1.19
PBiMA-6(3)	4.89	1.28	PBiA-6(3)	3.01	1.13
PBiMA-6(4)	5.86	1.32	PBiA-6(4)	4.11	1.14
PBiMA-6(5)	6.83	1.28	PBiA-6(5)	5.07	1.13
PBiMA-6(6)	8.78	1.31	PBiA-6(6)	5.47	1.13
PBiMA-6(7)	9.73	1.34			

a. Relative M_n and PDI were measured by GPC using PS standards.

3.2 Phase transitions and phase structures of the monomers and polymers

The phase structures of monomers were studied by POM and the results showed that all monomers only formed the crystalline phase (see **Figure S2**).

The thermal stability is an important property for potential applications. The TGA curves revealed that all PBiA-m showed good thermal stability (see **Figure S3**), that was, the temperatures at 5% weight loss of the samples under nitrogen were about 340 °C measured by TGA at a rate of 10 °C min^{-1} (see **Table 2**).

Fig.3 shows the second heating DSC curves of PBiA-m (m = 1, 4, 6, 10, 18) at a rate of 10 °C min^{-1} under nitrogen atmosphere after eliminating the thermal history. The high glass transition could be detected during the second heating progress and the results were shown in **Table 2**. In addition, the PBiA-18 presented the crystalline melting peaks of the long alkoxy tails in the low temperature.

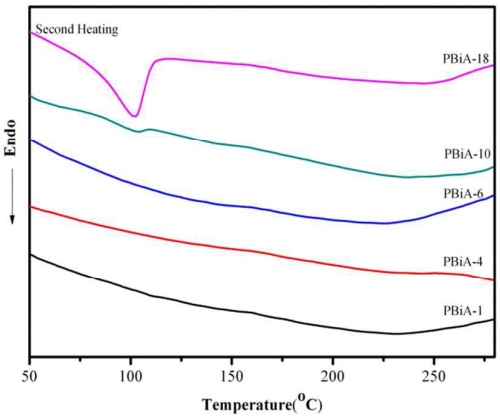

Fig.3 DSC curves of PBiA-m (m = 1, 4, 6, 10, 18) during the second heating scan at a rate of 10 °C min^{-1} under nitrogen atmosphere.

Table 2 Properties of PBiA-m (m = 1, 4, 6, 10, 18)

Sample	T_g (°C)[a]	T_d (°C)[b]	T_i (°C)[c]	2θ (°)[d]	*d*-spacing (nm)[d]	Calculated Length of the Mesogenic Units (nm)[e]
PBiA-1	190.3	379.9	—	3.49	2.55	1.395
PBiA-4	193.2	374.6	305.2	2.80	3.15	1.783
PBiA-6	171.1	340.3	301.0	2.65	3.33	2.032
PBiA-10	194.8	359.3	280.3	2.08	4.24	2.537
PBiA-18	172.4	362.1	299.8	1.52	5.81	3.545

a. The glass transition temperatures were measured by DSC at a heating rate of 10 °C min^{-1} under nitrogen atmosphere during the second heating process.

b. The temperatures at 5% weight loss of the samples under nitrogen [$T_d(N_2)$] were measured by TGA heating experiments at a rate of 20 °C min^{-1}.

c. The transition temperature from liquid crystalline phase to isotropic phase measured by POM at a heating rate of 10 °C min^{-1} during the second heating process.

d. Obtained from the 1D WAXD experiments.

e. Assuming the n-alkoxy tails in the side chains have an all-trans conformation.

Birefringence of the polymers is observed by POM. To get the perfect LC texture, all samples were heated to T_i except for PBiA-1, and then slowly cooled to the room temperature. The POM results of PBiA-4 and PBiA-18 were shown in **Fig.4** and the colour texture was observed, proving the formation of ordered structure. Through POM, we further observed the T_i of PBiA-m although it wasn't detected by DSC. The data was listed in **Table 2**, showing that PBiA-m presented the high T_i which exceeded to 280 °C.

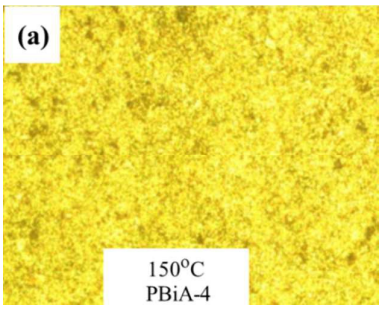

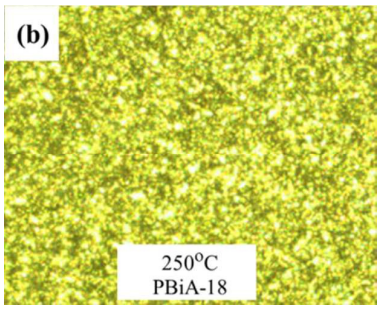

Fig.4 Representative POM images of the texture of the PBiA-4 maintained at 150 °C (a) and representative POM images of the texture of the PBiA-18 maintained at 200 °C (b) (Magnification: ×200).

In order to further study the phase structures of PBiA-m (m = 1, 4, 6, 10, 18), 1D WAXD experiments were performed and the results were shown in **Fig.5**. At room temperature, a strong reflection peak

and two weak reflection peaks were observed in the low angle for the PBiA-m. The ratio of scattering vectors of these peaks was 1: 2: 3, suggesting the polymer formed smectic phase. In the high angle, only an amorphous halo could be recognized. This reflected that no long range ordered structure formed via molecular packing was detected. To elucidate the packing of mesogens in the mesophase, the experimental interlayer distance was compared to the lamellar spacing L calculated using molecular modeling software from Material Studios 3.0. (L is the distance between a C-atom of the end-methyl group of the mesogen (full extended) and the carbon atom of the polymer chain). Through comparing the d-spacing with L (see **Table 2**), the PBiA-m (m = 1, 4, 6, 10, 18) formed a bilayer lamellar structure, in which the alkoxy tails were interdigitated in an antiparallel fashion.

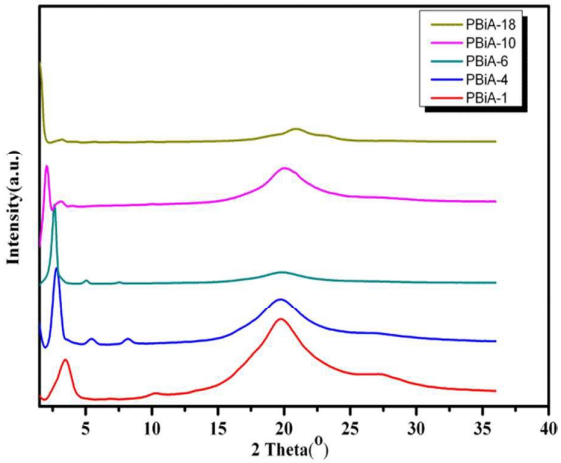

Fig.5 1D WAXD patterns of the PBiA-m (m = 1, 4, 6, 10, 18) at the room temperature.

On the other hand, the temperature-variable 1D WAXD experiments were performed. **Fig.6** illustrates the temperature-variable 1D WAXD patterns of PBiA-4 from 30 °C to 250 °C, implying that PBiA-4 exhibits the stable LC phase when heating or cooling. All other PBiA-m (m = 1, 6, 8, 18) showed similar 1D WAXD experiments results, suggesting the PBiA-m presented the stable smectic phase, which were consistent with POM results.

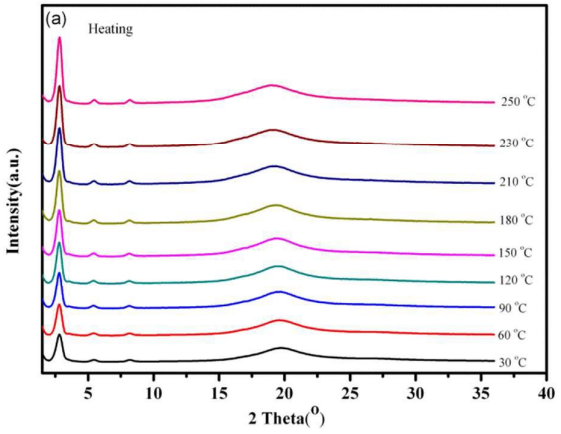

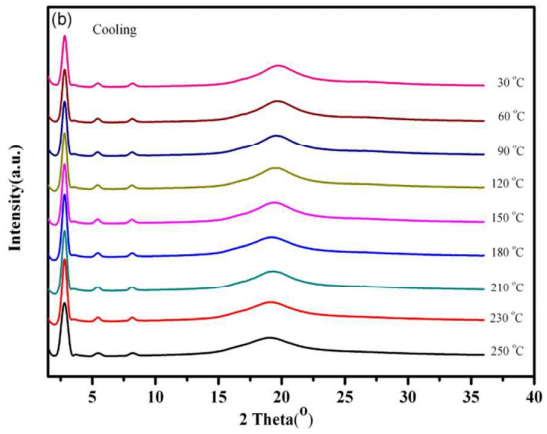

Fig.6 1D WAXD patterns of the PBiA-4 during the heating process (a) and the cooling process (b).

Based on the experiment results, the schematic of the smectic structure of PBiA-m was shown in **Fig.7**, indicating that the polymers formed the bilayer smectic structure in spite of the length of alkyl tail. What's more, with the increase of m, the spacing of layers of polymers increased from 2.55 nm to 5.81 nm.

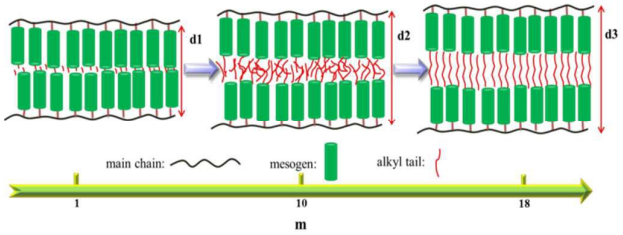

Fig.7 Possible liquid crystalline mesophase structures of PBiA-m.

For the polymers PBiA-m (m = 1, 4, 6, 8, 18) with low M_n which were synthesized via RAFT polymerization, the experiment results was similar to the polymers with high M_n which were synthesized via free radical polymerization, indicating that the M_n did not influence the phase behaviour and phase structure of polymers when the M_n reached to the low critical value. The POM results and properties of polymers were shown in **Figure S4** and **Table S1**, respectively. However, it should be noted that the PBiA-1 exhibited the lower T_i than the other polymers because it was easier to dissolve out from the reaction solution than the other polymers under the same reaction condition due to the short alkyl tail. With the increase of alkyl tail, the solubility property of polymers increases. Therefore, the PBiA-1 with lower M_n was prepared in order to make the polymer dissolve in solution, lead to the lower T_i.

3.3 Phase Transitions and Phase Structures of PBiMA-6(1) ~ PBiMA-6(7) and PBiA-6(1) ~ PBiA-6(6)

Fig.8 presents DSC curves of PBiMA-6(1) ~ PBiMA-6(7) and PBiA-6(1) ~ PBiA-6(6). As can be seen from **Fig.8** (a), the glass transition and a distinct transition peak related to the clearing transition were observed in the PBiMA-6(1) ~ PBiMA-6(7) and the

results were shown in **Table 3**. With the increasing of M_n, the T_g of the polymers increased from 101 °C to 184 °C and the Ti increased from 194 °C to 248 °C. For the PBiA-6, the DSC results were different from the PBiMA-6.

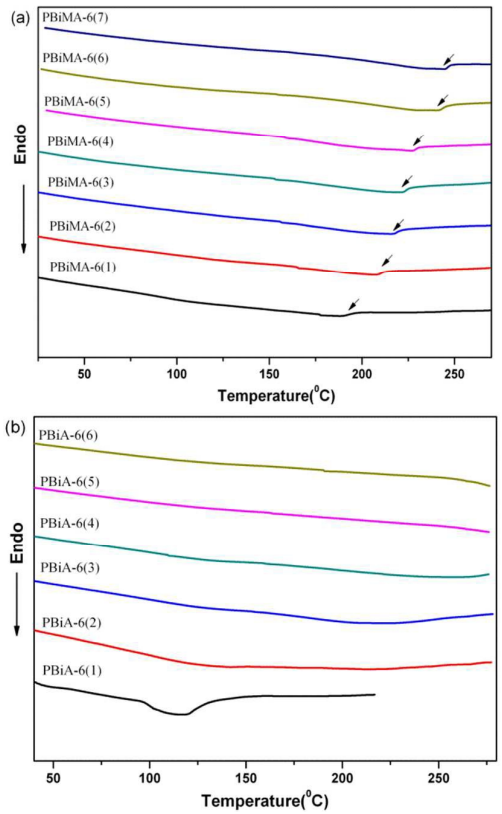

Fig.8 DSC curves of PBiMA-6(1) ~ PBiMA-6(7) (a) and PBiA-6(1) ~ PBiA-6(6) (b) during the second heating scan at a rate of 10 °C min^{-1} under nitrogen atmosphere.

From the **Fig.8** (b), a distinct transition peak related to T_i was observed for PBiA-6(1). For the PBiA-6(2) ~ PBiA-6(3), they only showed the glass transition (see **Table 3**). Lastly, no peak could be found in the PBiA-6(4) ~ PBiA-6(6).

For the PBiMA-6(1) ~ PBiMA-6(7), the needle-like texture could be seen, implying the formation of smectic phase (see **Fig.9** (a) and (b)). Meantime, the T_i increased with the increase of M_n and the results were consistent with DSC results. For the PBiA-6(1) ~ PBiA-6(6), the smectic schlieren texture was observed (see **Fig.9** (c) and (d)), corresponding to the formation of S_A phase. For the PBiA-6(5) and PBiA-6(6), the LC birefringence did not disappear until the samples were decomposed (300 °C). When cooled to room temperature from 300 °C, the birefringence of the sample remained the same, indicating that the ordered structure kept unchanged upon cooling.

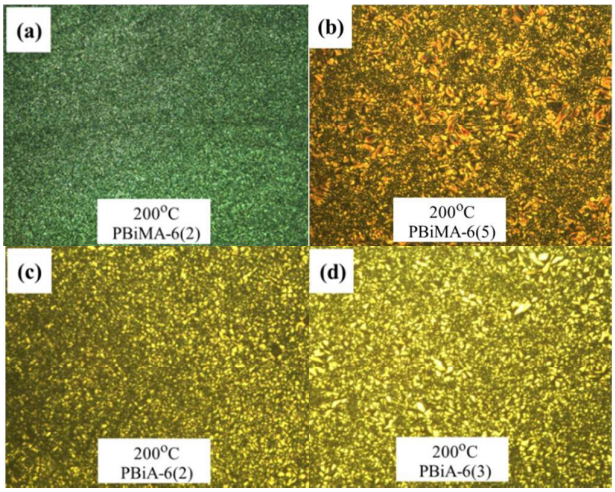

Fig.9 Representative POM images of the texture of the PBiMA-6(2) and PBiMA-6(5) maintained at 200 °C (a) and (b) and representative POM images of the texture of the PBiA-6(2) and PBiA-6(3) maintained at 200 °C (c) and (d) (Magnification: ×200).

Table 3 Properties of PBiMA-6(1) ~ PBiMA-6(7) and PBiA-6(1) ~ PBiA-6(6)

Sample	T_g (°C)[a]	T_i (°C)[a]	T_i (°C)[b]
PBiMA-6(1)	101.2	192.7	194
PBiMA-6(2)	116.9	209.7	204
PBiMA-6(3)	125.0	219.5	215
PBiMA-6(4)	136.0	223.8	225
PBiMA-6(5)	143.8	228.6	229
PBiMA-6(6)	178.7	243.2	244
PBiMA-6(7)	184.2	246.1	248
PBiA-6(1)	—	120.5	134
PBiA-6(2)	115.5	—	203
PBiA-6(3)	165.3	—	235
PBiA-6(4)	—	—	275
PBiA-6(5)	—	—	>300
PBiA-6(6)	—	—	>300

a. The transition temperature from liquid crystalline phase to isotropic phase measured by DSC at a heating rate of 10 °C min^{-1} under nitrogen atmosphere during the second heating process.

b. The transition temperature from liquid crystalline phase to isotropic phase measured by POM at a heating rate of 10 °C min^{-1} during the second heating process.

Fig.10 illustrates the 1D WAXD patterns of PBiMA-6(4) and PBiA-6(3). At low angle, three narrow reflection peaks are observed. The scattering vectors of these peaks are found to follow a ratio of 1: 2: 3, indicating a smectic structure with a periodicity of 3.21 nm and 3.27 nm, respectively. All other polymers showed the similar the 1D WAXD experiments results, demonstrating that the M_n showed little influence on the LC phase structure of the polymers.

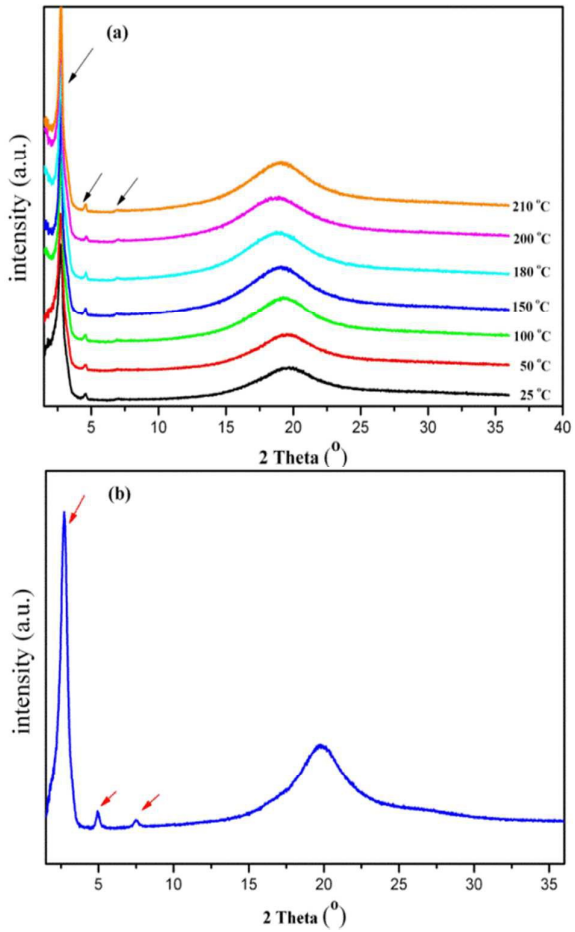

Fig.10 1D WAXD patterns of the PBiMA-6(4) during the heating process (a) and PBiA-6(3) at the room temperature (b).

In order to further confirm the phase transition and information about the nature of various phases, rheological measurements were carried out. The sample was loaded into the instrument at 160 °C. Temperature dependences of the shear storage modulus G', loss modulus G" and complex viscosity Eta* for PBiMA-6(5) were recorded at a rate of 10 °C min^{-1} in **Fig.11** (b). The transition temperatures evaluated by DSC at a rate of 10 °C min^{-1} in **Fig.11** (a). A peak shape of modulus and complex viscosity was seen around T_i, which agreed well with the transition temperature of this polymer on DSC scan. G', G" and Eta* decreased gradually with increasing temperature, and they steeply decreased with temperatures just below T_i. However, G', G" of Eta* changed scarcely above T_i. This maintenance in the isotropic phase was accounted for by the lesser mobility of the macromolecules. For the PBiA-6, the same results could be found (see **Fig.12**). Moreover, T_i was detected and the result was consistent with the POM, although it wasn't observed by DSC (see **Fig.8** (b)).

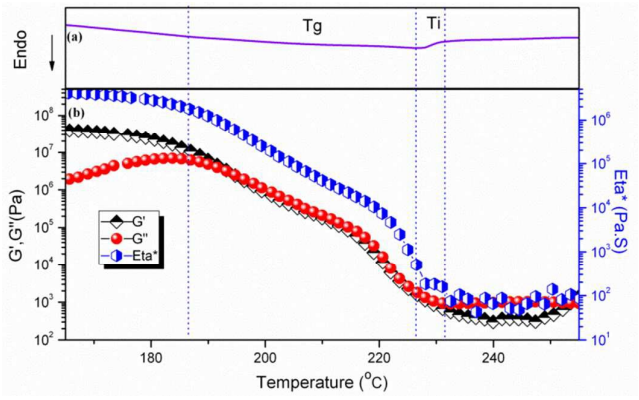

Fig.11 Heat flow at a heating rate 10 °C min^{-1} in DSC (a) and temperature dependence of G', G" and Eta* for during heating from 160 °C to 250 °C in rheology (b) for PBiMA-6(5). Conditions: 1% strain, 10 rad/s frequency and 10 °C min^{-1} heating rate.

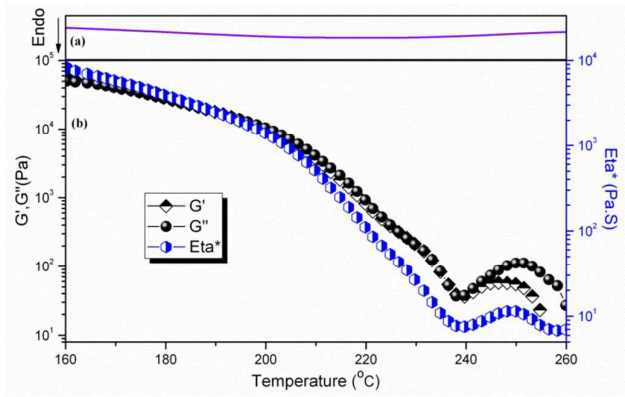

Fig.12 Heat flow at a heating rate 10 °C min^{-1} in DSC (a) and temperature dependence of G', G" and Eta* for during heating from 160 °C to 250 °C in rheology (b) for PBiA-6(3). Conditions: 1% strain, 10 rad s^{-1} frequency and 10 °C min^{-1} heating rate.

The moduli-frequency behavior of PBiMA-6(5) at various temperatures was shown in **Fig.13**. In the smectic A phase, the slope of G' against frequency was smaller than that of amorphous polymer melts, and the values of G' and G" were close to each other. Such behavior well reflected the high ordered packing structure of the side-chains in the smectic phase. This phenomenon also occurred in the smectic liquid crystalline side-chain polymers with the long spacer.[33] The shear viscosities of the PBiMA-6(5) at various temperatures was studied and the result was shown in **Figure S5**. For those temperature (185 °C to 205 °C), the viscosity-shear rate curves showed a shear thinning behavior over the shear rate range investigated and there was no sign of Newtonian plateau down to the lowest shear rate of 0.1 s^{-1}. For the PBiA-6, the same results were observed.

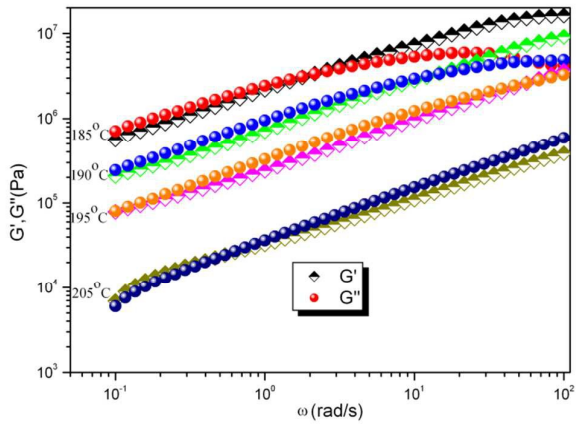

Fig.13 Frequency dependence of dynamic shear moduli for PBiMA-6(5) at various temperatures.

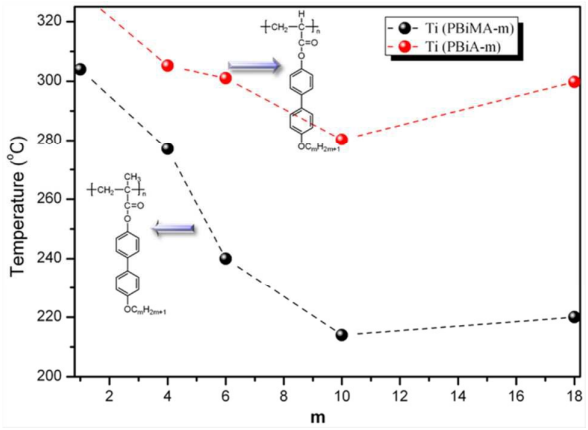

Fig.14 Dependence of clearing temperatures (T_i) on the number m of methylene groups in the tail for PBiMA-m and PBiA-m.

3.4 Influence of the main-chain and M_n on the Phase Behaviors

Based on DSC, POM and 1D WAXD experiments results, the dependence of the transition temperatures on m, for the PBiA-m and PBiMA-m was showed in **Fig.14**.[31] As can be seen from it, the both polymers exhibited the stable smectic A phase. There are two points to explain it. One point is that, when the alkoxy tails are added to the mesgoen, the interaction of mesgoen can increase due to the dipole-dipole interaction, leading to the formation of LC phase was developed by the mesgoens and the main chain. Another is that the main-chain is closely wrapped by the mesogens and is forced to stretch along the main-chain direction, leading to the stable LC phase. For the end-on SCLCPs with spacer, the polymers exhibited the smectic phase owing to the decoupling and self-organization of the mesgoen moieties. When heating, the flexible main-chain and flexible spacer strongly disturbed the order of mesgoens. On the other hand, the change of T_i has a similar tendency, that is, T_i decreases as the length of the alkyl tail increases and then increases slightly. We considered that the long flexible alkyl side chains was beneficial to the layered structures due to the unfavorable interaction between mesogens and the apolar alkyl side chains, leading to the stable of LC phase.

The differences between the PBiA-m and PBiMA-m are that, one aspect is solubility. For the PBiA-m, the M_n influences on solubility. The high M_n polymer synthesized by free radical polymerization could not be dissolved in the common solvent, while the low M_n polymer synthesized by RAFT polymerization showed good dissolvability, indicating that the interaction between the side-chains increased with the increase of M_n. For the PBiMA-m, the polymers with high or low M_n show good dissolvability. The second one is phase structure. When m varies, the phase structure of PBiMA-m will slightly change.[31] For the later, it only forms the bilayer smectic phase. The last point is transition temperature. The PBiMA-m and PBiA-m both exhibits the high T_i, but the PBiA-m shows the higher T_i than PBiMA-m.

Fig.15 displays the dependence of the transition temperatures on M_n, for the PBiMA-6 and PBiA-6. Through researching, we understand that, firstly, all polymers can form the bilayer smectic phase. Secondly, the T_i of PBiMA-6 and PBiA-6 increases with the increase of M_n. It is interesting that the Ti of PBiA-6 shows an S-curve dependence on M_n and the PBiA-6 has a higher T_i, compared to the PBiMA-6 with the similar M_n. The result is consistent with the high M_n via free radical polymerization (see **Fig.14**). As for this, it may be that the semiflexible main-chain (methacrylate main-chain) disturbs the ordered arrangement of mesgon when the temperature increases, contrast to the flexible main-chain (acrylate main-chain). Finally, compared with end-on SCLCPs with the alkyl spacer,[23, 28, 30] the PBiMA-6 and PBiA-6 exhibits the stable and simple LC phase structure.

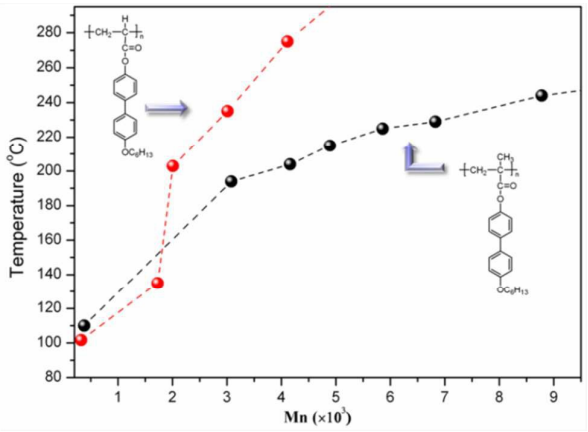

Fig.15 The relationship between the clearing temperatures (T_i) of PBiMA-6 and PBiA-6 and the M_n.

4. Conclusions

In summary, we have investigated the phase structures and transitions of poly(4, 4'-alkoxybiphenyl acrylate) (PBiA-m, m = 1, 4, 6, 10, 18) via DSC, POM and 1D WAXD. The results showed that

the PBiA-m exhibited the stable bilayer smectic A phase. Comparison of the properties of poly(4, 4'-alkoxybiphenyl acrylate) (PBiA-m) and poly(4, 4'-alkoxybiphenyl methacrylate) (PBiMA-m) demonstrated that the main-chain greatly influenced on the properties of SCLCPs without the spacer, containing the solubility, phase structure and phase transition temperature. In addition, we have synthesized two series of PBiMA-6 and PBiA-6 with narrow polydispersity by RAFT, and the phase behavior and structures of them were studies by DSC, POM, 1D WAXD and ARES rheometer. Both PBiMA-6 and PBiA-6 formed the bilayer semetic phase which was independence on the M_n of the polymers. With the increase of M_n, the T_i of PBiMA-6(1) ~ PBiMA-6(7) and PBiA-6(1) ~ PBiA-6(6) increased. However, compared with the PBiMA-6 with the similar M_n, the PBiA-6 had a higher T_i due to the flexible main-chain. The rheological properties showed that the steady shear viscosities of the smectic phase exhibited a shear thinning behavior over the shear rates investigated for PBiMA-6 and PBiA-6.

Acknowledgements

This research was financially supported by the National Nature Science Foundation of China (51373148).

Notes and references

1 V. Domenici, J. Milavec, A. Bubnov, D. Pociecha, B. Zupancic, A. Resetic, V. Hamplova, E. Gorecka, B. Zalar, *RSC Adv*., 2014, **4**, 44056.
2 G. Siva Mohan Reddy, T. Narasimhaswamy, K. Mohana Raju, *New. J. Chem*., 2014, **38**, 4357.
3 Y. Ryohei, K. Hideki, K. Yutaka, K. Sun-Nam, *Polymer*, 2014, 55, 1120.
4 J. F. Zheng, Z. Q. Yu, X. Liu, X. F. Chen, S. Yang, E. Q. Chen, *J. Polym. Sci. A. Polym. Chem*., 2012, **50**, 5023.
5 T. Tibor, C. Martin, F. Katalin, H. Věra, J., István K. Miroslav, V., Terezia H. František, B. Alexej, *Macromol. Chem. Phys.*, 2014, **215**, 742.
6 X. Q. Liu, J. Wang, S. Yang, E. Q., *Macro. Lett.*, 2014, **3**, 834.
7 E. Perplies, H. Ringsdorf, J. H. Wendorff, *Die. Makromolekulare. Chemie.* 1974, **175**, 5531.
8 V. P. Shibaev, N. A. Plat, *Adv. Polym. Sci.*, 1984, **60-61**, 173.
9 P. Giovanna, M. Pierluigi, G. Paolo, *J. Polym. Sci. A. Polym. Chem.* 1971, **9**, 1133.
10 P. L. Magagninla, G. Pizzirani, G. Turchi, *Eur. Polym. J.*, 1974, **10**, 585.
11 E. C. Hsu, S. B. Clough, A. Blumstein, *J. Polym. Sci. Polym. Lett. Ed.*, 1977, **15**, 545.
12 H. Finkelmann, H. Ringsdorf, J. H. Wendorff, *Makromol. Chem.*, 1978, **179**, 273.
13 H. Finkelmann, G. Rehage, *Adv. Polym. Sci.*, 1984, **60-61**, 97.
14 G. Tomasz, S. Włodzimierz, *Materials*, 2009, **2**, 95.
15 Y. Zhou, V. A. Briand, N. Sharma, S. Ahn, R. M. Kasi, *Materials*, 2009, **2**, 636.
16 A. A. Craig, C.T. Imrie, *Macromolecules*, 1995, **28**, 3617.
17 A. G. Cook, R.T. Inkster, A. Martinez-Felipe, A. Ribes-Greus, I. W. Hamley, C.T. Imrie, *Eur. Polym. J.* 2012, **48**, 821.
18 X. Li, L. Fang, L. Hou, L. Zhu, Y. Zhang, B. Zhang, H. Zhang, *Soft Matter*, 2012, **8**, 5532.
19 X. Q. Zhu, J. H. Liu, Y. X. Liu, E. Q. Chen, *Polymer*, 2008, **49**, 3103.
20 F. Stephan, L. L. Francüois, R. Paul, N. Almeria, *Macromolecules*, 2003, **36**, 2680.
21 V. Percec, D. Tomazos, *Adv. Mater.*, 1992, **4**, 548.
22 V. Percec, D. Schlueter, Y. K. Kwon, J. Blackwell, M. Moller, P. J. Slangen, *Macromolecules*, 1995, **28**, 8807.
23 X. Hao, J. P. A. Heuts, C. Barner-Kowollik, T. P. Davis, *J. Polym. Sci. A. Polym. Chem*., 2003, **41**, 2949.
24 C. S. Hsu, V. Percec, *Polym. Bull.*, 1987, **17**, 49.
25 B. Hahn, V. Percec, *Macromolecules*, 1987, **20**, 2961.
26 D. Wu, B. Ni, Y. Liu, S. Chen, H. L. Zhang, *J. Mater. Chem. A.*, 2015, **3**, 9645.
27 V. Percec, M. Lee, *Macromolecules*, 1991, **24**, 2780.
28 N. Tomikawa, T. Itoh, Y. Okazaki, M. Adachi, M. Tokita, J. Watanabe, *Jpn. J. Appl. Phys.*, 2005, **44,** 381.
29 N. Boiko, V. Shibaev, B. Ostrovskii, S. Sulyanov, D. Wolff, J. Springer, *Macromol. Chem. Phys.*, 2001, **202**, 297.
30 V. Percec, M. Lee, *Macromolecules*, 1991, **24**, 1017.
31 B. Ni, J. Q. Liao, S. Chen, H. L. Zhang, *RSC Adv.*, 2015, **5**, 9035.
32 H. B. Li, B. Yu, H. Matsushima, C. E. Hoyle, A. B. Lowe, *Macromolecules*, 2009, **42**, 6537.
33 I. K. Yang, S. H. Chang, *J. Polym. Res.*, 2002, **9**, 163.